

Antifungal Polymer Containing Menthoxy Triazine

Xuefei Li,[#] Zixu Xie,[#] Guofeng Li, Lei Tao, Yen Wei, and Xing Wang*Cite This: <https://doi.org/10.1021/acsapm.1c00506>

Read Online

ACCESS |



Metrics & More



Article Recommendations



Supporting Information

ABSTRACT: An antifungal polymer containing menthoxy triazine was synthesized by a polycondensation of 2,4-dichloro-6-menthoxy-1,3,5-triazine (DMT) with 4,4-oxidianiline (ODA) and named as P(MT-*alt*-ODA). To emphasize the antifungal performance of the menthoxy group, series of similar triazine polymers derived correspondingly with hydrogen, ethoxy, and decoxy groups were prepared and served as controls. The spores of *Aspergillus niger* were used for an antifungal evaluation. Only P(MT-*alt*-ODA) can effectively inhibit the growth and spread of spores. A further in-depth analysis combined with an inhibition zone and water contact angle illustrated that the surface menthoxy stereochemistry is crucial for the antifungal mechanism.

KEYWORDS: antifungal polymer, menthoxy triazine, stereochemical antifungal strategy, managing and controlling microorganisms, fungal contamination, spore behaviors



INTRODUCTION

Fungal contamination causes huge economic losses in many fields,^{1,2} and its infections have become one of the most serious risks to human health. Millions of people are suffering from invasive fungal infections, and more than 50% of them die each year.^{3,4} The main reason for these hazards is the rapid spread and propagation of fungi.^{5,6} Therefore, if fungal spread and propagation can be controlled, the harm caused by fungal infections can be greatly reduced. However, since airborne fungi spores are almost everywhere, it is still difficult for many materials to restrict the colonization and activity of fungal spores.

Traditional antifungal materials achieve efficient fungicidal ability usually by releasing fungicides such as antibiotics, quaternary ammonium compounds,⁷ and heavy metals,^{8,9} but the concentration of those fungicides will decrease over time, resulting in a reduction in antifungal efficiency.^{10,11} Besides, the abuse of fungicides will accelerate the process of drug resistance, which continues to grow and evolve worldwide, resulting in the failure of antifungal therapy.^{12,13} What's more, conventional fungicides may be seriously toxic to cells or even harmful for the intrinsic flora of the human body. So, it is an advance to produce nonreleasing materials that can prevent the spread of spores, rather than kill them according to the consideration of toxicity risk.

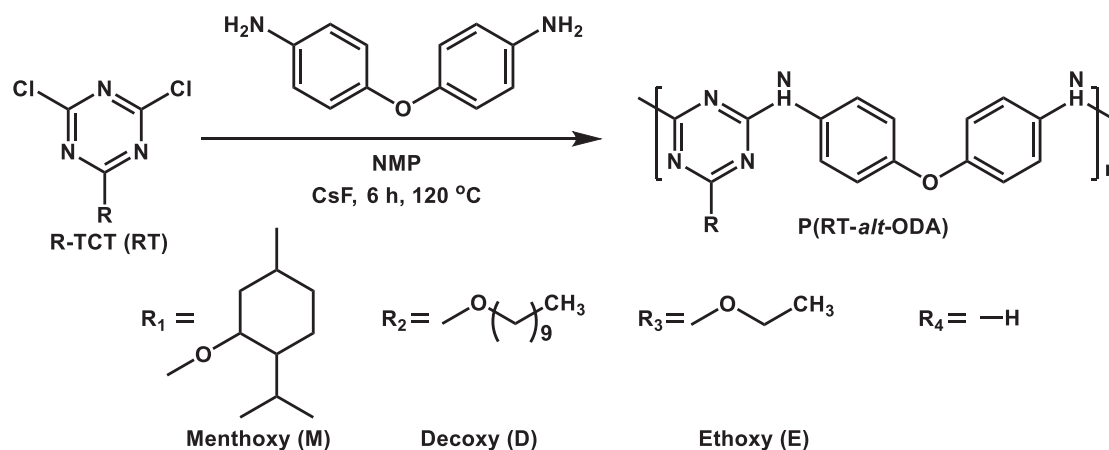
Menthol is a natural plant-derived compound. It has been used as a green antimildew bacteriostatic agent.^{14,15} We noticed it because it has a ring-like molecular structure,^{16,17} making it a potential candidate for stereochemical antifungal materials.¹⁸ This kind of material can effectively limit the invasion of fungi to the surface of the material mainly because

of the covalent bonding of steric molecules rather than the release of fungicides. Thus, a covalent modification with menthol should be an appropriate method to obtain antifungal materials. 2,4,6-Trichloro-1,3,5-triazine (TCT), which is inexpensive and commercially available,¹⁹ is a suitable carrier for a polymer synthesis,²⁰ because it can be substituted in a proper sequence by the functional groups of $-OH$, $-NH$, and $-SH$ to form triazine derivatives.^{21,22} Therefore, the combination of menthol and TCT will hopefully create an ideal stereochemical antifungal material.

Herein, we present our work on an antifungal polymer containing menthoxy triazine (see R_1 in Scheme 1), which was synthesized by the copolycondensation of 2,4-dichloro-6-menthoxy-1,3,5-triazine (DMT) and 4,4-oxidianiline (ODA). It is named as P(MT-*alt*-ODA) (R_1) to compare with the control groups of P(DT-*alt*-ODA) (R_2), P(ET-*alt*-ODA) (R_3), and P(T-*alt*-ODA) (R_4), where MT, DT, ET, and T are short for menthoxy triazine, decoxy triazine, ethoxy triazine, and triazine, respectively. The antifungal activity of all four polymers against *Aspergillus niger* was investigated with the designed Prison Break test (described below). The superiority of P(MT-*alt*-ODA) in inhibiting the spread and growth of

Received: April 22, 2021

Accepted: June 30, 2021

Scheme 1. Synthesis of the Antifungal Polymer P(MT-*alt*-ODA) (R_1)^a

^aP(DT-*alt*-ODA) (R_2), P(ET-*alt*-ODA) (R_3), and P(T-*alt*-ODA) (R_4) are control groups. DT, ET, T, and MT are short for decoxy triazine, ethoxy triazine, triazine, and menthoxy triazine, respectively.

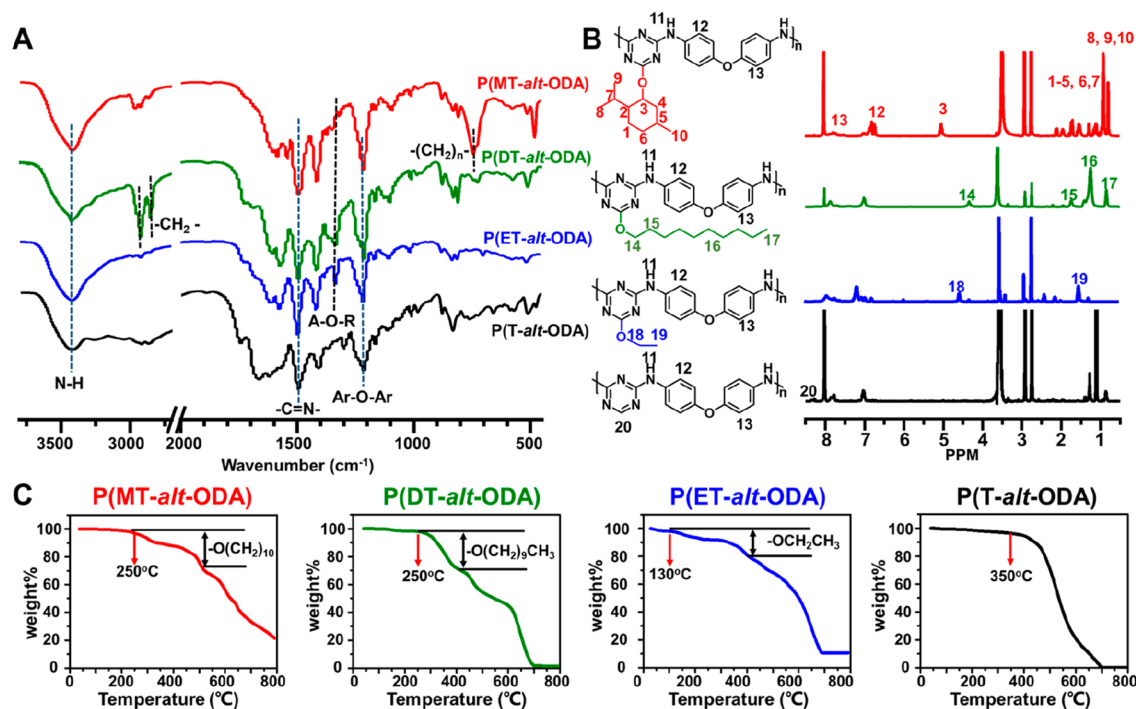


Figure 1. (A) FT-IR spectra, (B) ¹H NMR spectra, and (C) TGA test of the four polymers. Red, P(MT-*alt*-ODA); green, P(DT-*alt*-ODA); blue, P(ET-*alt*-ODA); black, P(T-*alt*-ODA).

fungal spores, or working as molecular prison of spores, was demonstrated.

The chemical structures of P(MT-*alt*-ODA), P(DT-*alt*-ODA), P(ET-*alt*-ODA), and P(T-*alt*-ODA) were first checked by Fourier transform infrared spectroscopy (FT-IR; Figure 1A). The absorption band characteristic of stretching vibrations of the TCT ($-C=N-$) group was observed at 1500 cm^{-1} . Bands corresponding to the aromatic ether ($-O-Ar$) groups of the four polymers can be detected at 1210 cm^{-1} . In addition, the absorption peaks of the ether ($-O-R$) group of the P(MT-*alt*-ODA), P(DT-*alt*-ODA), and P(ET-*alt*-ODA) were found at $1330\text{--}1350\text{ cm}^{-1}$. The characteristic band at 742 cm^{-1} for $-(CH_2)_n-$ stretching vibrations from menthoxy groups was also registered. Moreover, the strong absorption bands at 3421 cm^{-1} of four polymers were assigned to the free

N-H stretching absorption. All these results indicate that the desired functional groups appeared on the four polymers.

Further qualitative analysis was performed by obtaining ¹H NMR spectra; they were shown in Figure 1B with all peak assignments marked. For the P(T-*alt*-ODA) (Figure 1B, black), there is no characteristic peak at $\delta = 4\text{--}5.5\text{ ppm}$ compared to that on the spectra of P(MT-*alt*-ODA) (Figure 1B, red), P(DT-*alt*-ODA) (Figure 1B, green), and P(ET-*alt*-ODA) (Figure 1B, blue), while the characteristic peaks in this interval were assigned to the hydrocarbon groups that attached to the oxygen atoms in the polymer side chains of P(MT-*alt*-ODA), P(DT-*alt*-ODA), and P(ET-*alt*-ODA) (3, 14, 18 in Figure 1B). In addition, the integral area ratio of other groups on the side chain can also be correspondence. The assigned peak at $\delta = 7.05\text{ ppm}$ represented the benzene ring (12, 13 in

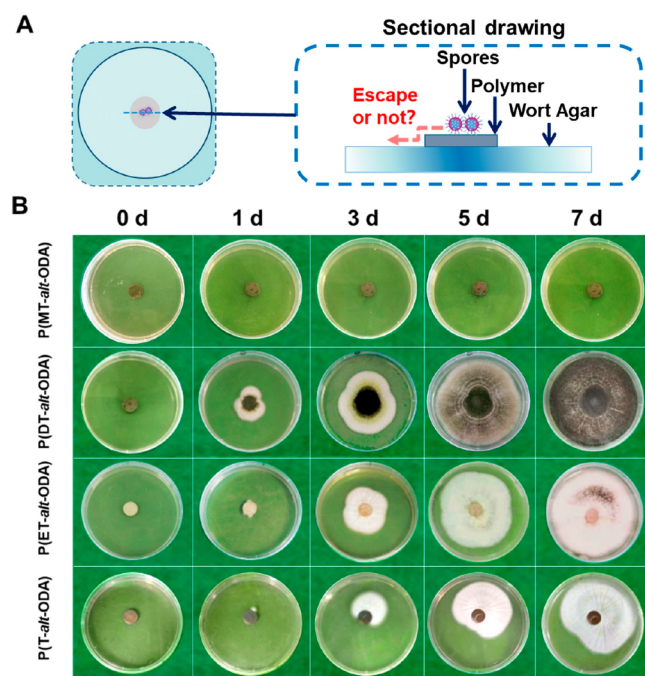


Figure 2. (A) Schematic illustration of a modified Prison Break test for an antifungal adhesion assay of polymers; (B) Prison Break tests of P(MT-*alt*-ODA), P(DT-*alt*-ODA), P(ET-*alt*-ODA), and P(T-*alt*-ODA).

Figure 1B). Combined with the FT-IR and ^1H NMR characterizations, it can be proved that the required polymers were synthesized successfully.

A thermogravimetric analysis (TGA) test presents the thermal properties of the four polymers. As it is shown in Figure 1C, a weight loss of 2–5% from 25 to 130 °C is mainly due to the loss of absorbed water. In terms of P(MT-*alt*-ODA), P(DT-*alt*-ODA), and P(ET-*alt*-ODA), the first section of the descending curve is caused by the removal of the covalently linked menthoxy, decoxy, and ethoxy groups, which correspond to the temperatures of 500, 400, and 400 °C, respectively.^{23–26} In detail, for polymer P(MT-*alt*-ODA), the weight loss of ~34.7% (including ~2% of absorbed water loss) at 500 °C is consistent with the weight of the menthoxy group of P(MT-*alt*-ODA).²³ In addition, for P(DT-*alt*-ODA) (molecular weight of 470.03), the decoxy unit (molecular weight of 158.29) accounts for 33% of the total mass. Thus, the weight loss of ~35% at 400 °C is exactly the weight loss of the *n*-decyl alcohol unit,²⁴ regardless of the ~2% weight loss of the absorbed water. For P(ET-*alt*-ODA) (molecular weight of 402.58), the ethoxy unit (with the molecular weight of 46.07) accounts for 11.1% of the overall mass. The weight loss of 15% at 400 °C with ~4% absorbed water weight loss is consistent with the weight loss of the ethanol unit precisely.²⁵ For P(MT-*alt*-ODA) the descending curve between 500 and 670 °C is due to the covalently linked TCT removal. At the same time, for P(DT-*alt*-ODA) and P(ET-*alt*-ODA), the descending curve is due to the covalently linked TCT removal between 400 and 500 °C. The above data showed that P(MT-*alt*-ODA) had the best thermal stability among the four polymers.

The gel permeation chromatography (GPC) test was performed to further prove that the four polymers were synthesized successfully. The results show that the molecular weights of the four polymers were above 10^3 , among which the

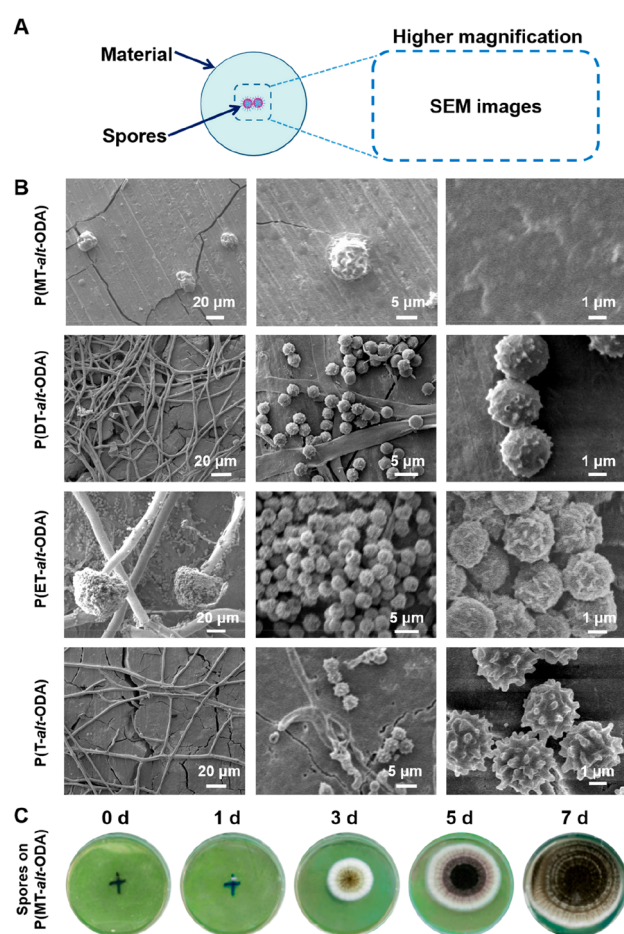


Figure 3. (A) Schematic illustration of the sampling point of SEM images. (B) SEM images of the P(MT-*alt*-ODA), P(DT-*alt*-ODA), P(ET-*alt*-ODA), and P(T-*alt*-ODA) Prison Break test 7 d later. (C) Determination of the spore activity on materials after 7 d of the Prison Break test of P(MT-*alt*-ODA).

molecular weight of P(MT-*alt*-ODA) reached 10^4 (Figure S3 and Table S1). In addition, the polydispersity index (PDI) values of the four groups of polymers are all in the range of 1.1–1.3, indicating the narrow distribution of relative molecular mass. The above results further prove that the four polymers were synthesized successfully. Next, we attempted to elucidate the effect of different structural modifications on the antifungal effect of materials through the modified Prison Break test. The Prison Break test was first designed for the evaluation of the antibacterial adhesion activity of materials.²⁷ This is a naked eye visualization method, and it is easy to implement. Then, the Prison Break test was modified for the antifungal evaluation. The modified Prison Break model consists of three parts: wort agar medium, polymer material, and fungal spores (Figure 2A). The polymer material was placed on the surface of wort agar medium. Then, fungal spores were placed on the center of the material. After an incubation at 30 °C, the growth of spores was photographed by a camera every 24 h. The antifungal activities of materials were evaluated by the time spores broke through the restriction of the material and grew on the wort agar medium. The modified Prison Break test showed that the fungi spores “escaped” from the surface of the P(DT-*alt*-ODA), P(ET-*alt*-ODA), and P(T-*alt*-ODA) tablets and grew on the wort

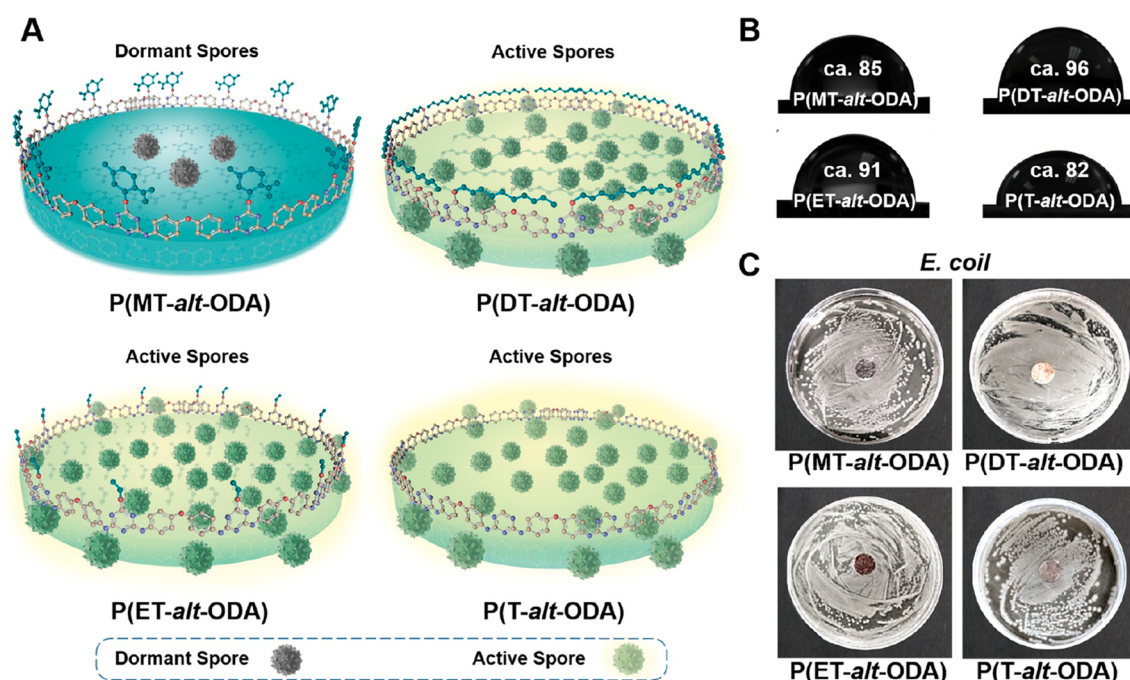


Figure 4. (A) Antifungal ability model of polymers. (B) CA measurements on polymers. Data values correspond to mean \pm standard deviation ($n = 3$). (C) Inhibition zone test of antifungal polymers against *E. coli*.

medium after 1 d of incubation, suggesting that the P(DT-*alt*-ODA), P(ET-*alt*-ODA), and P(T-*alt*-ODA) showed no antifungal activity against fungi proliferation and diffusion. In contrast, the P(MT-*alt*-ODA) limited the fungi spore within the tablet for a week, demonstrating the perfect antifungal ability to inhibit the growth and diffusion of *A. niger* (Figure 2B). These results manifest that the unique stereochemical structure of menthoxy group exhibits great advantages in antifungal properties.

In order to determine whether P(MT-*alt*-ODA) inhibited the germination of *A. niger* spores or killed it, the scanning electron microscope (SEM) was used to observe the morphology of spores on the surface of the materials that were cultured for 7 d in the Prison Break test. The SEM images showed that morphologies of spores were different from each other (Figure 3B). Besides, large amounts of hyphae grew out on the surfaces of P(DT-*alt*-ODA), P(ET-*alt*-ODA), and P(T-*alt*-ODA). In contrast, no hyphae grew on the P(MT-*alt*-ODA), and no spore was observed on the edge of the P(MT-*alt*-ODA) tablet even at a high magnification (the right image in Figure 3B). This was good evidence that P(MT-*alt*-ODA) can effectively inhibit the growth of spores. However, it is still uncertain whether the spores on the surface of P(MT-*alt*-ODA) had been killed or just stayed dormant. To figure this out, a new test was introduced. The P(MT-*alt*-ODA) tablet from the Prison Break test after 7 d was transferred into a new wort medium, with the spore side down (Figure 3C), and then the tablet was removed after 10 s. At this point, spores on the material had been transferred to the medium and then cultured at 30 °C. After 7 d of incubation, the *A. niger* grew up on the medium (Figure 3C), indicating that P(MT-*alt*-ODA) just inhibited the germination of *A. niger* spores instead of killing them.

Obviously, it can be concluded that P(MT-*alt*-ODA) can effectively limit the fungal spores to the surface of a material without spreading and germinating. The excellent antifungal

ability of P(MT-*alt*-ODA) should be due to the unique stereochemical structure of the menthoxy unit, which trapped the fungal spores in it like a molecular prison of spores (Figure 4A). However, linear stereochemical structure units in P(DT-*alt*-ODA) and P(ET-*alt*-ODA) have no such effect. They cannot inhibit the growth and spread of fungi (Figure 4A), although the decoxy group has the same number of carbon atoms as the menthoxy group.

Previous works have proved that the hydrophilicity and hydrophobicity of materials will affect their antimicrobial properties.²⁸ Additionally, P(MT-*alt*-ODA), P(DT-*alt*-ODA), P(ET-*alt*-ODA), and P(T-*alt*-ODA) showed similar hydrophobicity with the water contact angle (CA) of $85 \pm 2^\circ$, $96 \pm 3^\circ$, $91 \pm 4^\circ$, and $82 \pm 4^\circ$, respectively (Figure 4B). The slight increase in CA in the order of P(T-*alt*-ODA), P(ET-*alt*-ODA), and P(DT-*alt*-ODA) can be attributed to the regularly increasing length of the alkyl chain, and the longer of the alkyl chain, the stronger the hydrophobicity of the stationary phase is. However, the differences in CA are negligible, and the hydrophobic properties of the four materials were very similar, so the antifungal ability of P(MT-*alt*-ODA) is independent of the hydrophobicity.

The zone of inhibition test is usually used to characterize the ability of a material to kill microorganisms by releasing germicides. Experiments showed that the four polymers did not show any inhibition zone in any of the studied materials (P(MT-*alt*-ODA), P(DT-*alt*-ODA), P(ET-*alt*-ODA), and P(T-*alt*-ODA)) against *Escherichia coli*. The polymers did not release any germicides, which indicates that these four materials are nonreleasing materials. All these results indicate that the antimicrobial activity of P(MT-*alt*-ODA) was due to the unique surface stereochemistry of the menthoxy unit.

CONCLUSION

In summary, we had synthesized a type of antifungal polymer P(MT-*alt*-ODA). The polymer was hydrophobic and had

stable thermodynamic properties. It is worth mentioning that it exhibited an effective suppression on the spread and germination of fungal spores without killing them. The long-term antifungal activities were attributed to the surface stereochemical selectivity of fungi rather than the hydrophobic selectivity. The menthoxy polymer P(MT-*alt*-ODA) forms a molecular prison of spores, where the fungi were firmly confined. The menthoxy polymer is a candidate of a stereochemical antifungal strategy^{18,29,30} and will be promising for managing and controlling microorganisms. This strategy can effectively limit fungi landing on the materials surface, so as to prevent fungal contaminations.

■ ASSOCIATED CONTENT

SI Supporting Information

The Supporting Information is available free of charge at <https://pubs.acs.org/doi/10.1021/acsapm.1c00506>.

Materials, experimental procedures, ¹H NMR spectra of monomers, GPC results (PDF)

■ AUTHOR INFORMATION

Corresponding Author

Xing Wang – Beijing Laboratory of Biomedical Materials, College of Life Science and Technology, Beijing University of Chemical Technology, Beijing 100029, China; orcid.org/0000-0002-9990-1479; Phone: +86-10-64416428; Email: wangxing@mail.buct.edu.cn

Authors

Xuefei Li – Beijing Laboratory of Biomedical Materials, College of Life Science and Technology, Beijing University of Chemical Technology, Beijing 100029, China; Baotou Research Institute of Rare Earths, Baotou 014030, China

Zixu Xie – Beijing Laboratory of Biomedical Materials, College of Life Science and Technology, Beijing University of Chemical Technology, Beijing 100029, China

Guofeng Li – Beijing Laboratory of Biomedical Materials, College of Life Science and Technology, Beijing University of Chemical Technology, Beijing 100029, China

Lei Tao – The Key Laboratory of Bioorganic Phosphorus Chemistry & Chemical Biology (Ministry of Education), Department of Chemistry, Tsinghua University, Beijing 100084, China; orcid.org/0000-0002-1735-6586

Yen Wei – The Key Laboratory of Bioorganic Phosphorus Chemistry & Chemical Biology (Ministry of Education), Department of Chemistry, Tsinghua University, Beijing 100084, China; orcid.org/0000-0001-5950-0163

Complete contact information is available at: <https://pubs.acs.org/doi/10.1021/acsapm.1c00506>

Author Contributions

[#]X.-F. L. and Z.-X. X. contributed equally to this work.

Notes

The authors declare no competing financial interest.

■ ACKNOWLEDGMENTS

The authors are thankful for the financial support provided by the National Natural Science Foundation of China (No. 21574008).

■ REFERENCES

- (1) Dadzie, M.; Oppong, A.; Ofori, K.; Eleblu, J.; Ifie, E.; Blay, E.; Obeng-Bio, E.; Appiah-Kubi, Z.; Warburton, M. Distribution of *Aspergillus Flavus* and aflatoxin accumulation in stored maize grains across three agro-ecologies in Ghana. *Food Control* **2019**, *104*, 91–98.
- (2) Liu, Q.; Sun, K.; Zhao, N.; Yang, J.; Zhang, Y.; Ma, C.; Pan, L.; Tu, K. Information fusion of hyperspectral imaging and electronic nose for evaluation of fungal contamination in strawberries during decay. *Postharvest Biol. Technol.* **2019**, *153*, 152–160.
- (3) Brown, G.; Denning, D.; Gow, N.; Levitz, S.; Netea, M.; White, T. Hidden killers: human fungal infections. *Sci. Transl. Med.* **2012**, *4* (165), 165rv13–165rv13.
- (4) Perfect, J. The antifungal pipeline: a reality check. *Nat. Rev. Drug Discovery* **2017**, *16*, 603–616.
- (5) Latge, J. P. *Aspergillus fumigatus* and aspergillosis. *Clin. Microbiol. Rev.* **1999**, *12* (2), 310–350.
- (6) Li, Z.; Lu, G.; Meng, G. Pathogenic fungal infection in the lung. *Front. Immunol.* **2019**, *10*, 1524.
- (7) Hsu, L.; Kwaśniewska, D.; Wang, S.; Shen, T.; Wieczorek, D.; Chen, Y. Gemini quaternary ammonium compound PMT12-BF4 inhibits *Candida albicans* via regulating iron homeostasis. *Sci. Rep.* **2020**, *10* (1), 1–12.
- (8) Robles-Martínez, M.; Patiño-Herrera, R.; Pérez-Vázquez, F. J.; Montejano-Carrizales, J.; González, J.; Pérez, E. *Mentha piperita* as a natural support for silver nanoparticles: a new anti-*Candida albicans* treatment. *Colloid Interface Sci. Commun.* **2020**, *35*, 100253.
- (9) Guerra, J.; Sandoval, G.; Avalos-Borja, M.; Pestryakov, A.; Garibo, D.; Susarrey-Arce, A.; Bogdanchikova, N. Selective antifungal activity of silver nanoparticles: a comparative study between *Candida tropicalis* and *Saccharomyces boulardii*. *Colloid Interface Sci. Commun.* **2020**, *37*, 100280.
- (10) Cioffi, N.; Torsi, L.; Ditaranto, N.; Tantillo, G.; Ghibelli, L.; Sabbatini, L.; Blevé-Zacheo, T.; D'Alessio, M.; Zamboni, P.; Traversa, E. Copper nanoparticle/polymer composites with antifungal and bacteriostatic properties. *Chem. Mater.* **2005**, *17* (21), 5255–5262.
- (11) Cioffi, N.; Torsi, L.; Ditaranto, N.; Sabbatini, L.; Zamboni, P.; Tantillo, G.; Ghibelli, L.; D'Alessio, M.; Blevé-Zacheo, T.; Traversa, E. Antifungal activity of polymer-based copper nanocomposite coatings. *Appl. Phys. Lett.* **2004**, *85* (12), 2417–2419.
- (12) Pfaller, M. A. Antifungal drug resistance: mechanisms, epidemiology, and consequences for treatment. *Am. J. Med.* **2012**, *125* (1), S3–S13.
- (13) Anderson, J. B. Evolution of antifungal-drug resistance: mechanisms and pathogen fitness. *Nat. Rev. Microbiol.* **2005**, *3* (7), 547–556.
- (14) Patil, R.; Nimbalkar, M.; Jadhav, U.; Dawkar, V.; Govindwar, S. Antiaflatoxic and antioxidant activity of an essential oil from *Ageratum conyzoides* L. *J. Sci. Food Agric.* **2010**, *90* (4), 608–614.
- (15) Naeini, A.; Ziglari, T.; Shokri, H.; Khosravi, A. Assessment of growth-inhibiting effect of some plant essential oils on different *Fusarium* isolates. *J. Mycol. Med.* **2010**, *20* (3), 174–178.
- (16) Edris, A.; Derivatives, T. Pharmaceutical and therapeutic potentials of essential oils and their individual volatile constituents: a review. *Phytother. Res.* **2007**, *21* (4), 308–323.
- (17) Trombetta, D.; Castelli, F.; Sarpietro, M. G.; Venuti, V.; Cristani, M.; Daniele, C.; Saija, A.; Mazzanti, G.; Bisignano, G. Mechanisms of antibacterial action of three monoterpenes. *Antimicrob. Agents Chemother.* **2005**, *49* (6), 2474–2478.
- (18) Xu, J.; Xie, Z.; Du, F.; Wang, X. One-step anti-superbug finishing of cotton textiles with dopamine-menthol. *J. Mater. Sci. Technol.* **2021**, *69*, 79–88.
- (19) Blotny, G. Recent applications of 2, 4, 6-trichloro-1, 3, 5-triazine and its derivatives in organic synthesis. *Tetrahedron* **2006**, *62* (41), 9507–9522.
- (20) Saito, K.; Nishimura, N.; Sasaki, S.; Oishi, Y.; Shibasaki, Y. Synthesis of polyguanamines from 2-N, N-dibutylamino-4, 6-dichloro-1, 3, 5-triazine with aromatic diamines. *React. Funct. Polym.* **2013**, *73* (5), 756–763.

- (21) Figg, C.; Kubo, T.; Sumerlin, B. Efficient and chemoselective synthesis of ω , ω -heterodifunctional polymers. *ACS Macro Lett.* **2015**, *4* (10), 1114–1118.
- (22) Kubo, T.; Figg, C.; Swartz, J.; Brooks, W.; Sumerlin, B. Multifunctional homopolymers: postpolymerization modification via sequential nucleophilic aromatic substitution. *Macromolecules* **2016**, *49* (6), 2077–2084.
- (23) Jiang, T. Y.; Zhang, B. Y.; Tian, M.; Wang, Y. Synthesis and characterization of chiral side-chain liquid-crystalline polymer containing menthol ester. *J. Appl. Polym. Sci.* **2003**, *89* (10), 2845–2851.
- (24) Zimmermann, I.; Urieta-Mora, J.; Gratia, P.; Aragó, J.; Grancini, G.; Molina-Ontoria, A.; Ortí, E.; Martín, N.; Nazeeruddin, M. K. High-efficiency perovskite solar cells using molecularly engineered, thiophene-rich, hole-transporting materials: influence of alkyl chain length on power conversion efficiency. *Adv. Energy Mater.* **2017**, *7* (6), 1601674.
- (25) Sung, J. H.; Choi, H. Electrorheological characteristics of poly(o-ethoxy)aniline nanocomposite. *Korea-Aust Rheol J.* **2004**, *16* (4), 193–199.
- (26) Wang, J.; Harrison, M. Removal of organic micro-pollutants from water by β -cyclodextrin triazine polymers. *J. Inclusion Phenom. Macrocyclic Chem.* **2018**, *92* (1–4), 347–356.
- (27) Luo, L.; Li, G.; Luan, D.; Yuan, Q.; Wei, Y.; Wang, X. Antibacterial adhesion of borneol-based polymer via surface chiral stereochemistry. *ACS Appl. Mater. Interfaces* **2014**, *6* (21), 19371–19377.
- (28) Wang, Y.; Shen, J.; Yuan, J. Design of hemocompatible and antifouling PET sheets with synergistic zwitterionic surfaces. *J. Colloid Interface Sci.* **2016**, *480*, 205–217.
- (29) Xie, Z.; Li, G.; Wang, X. Chiral stereochemical strategy for antimicrobial adhesion. In *Racing for the Surface: Pathogenesis of Implant Infection and Advanced Antimicrobial Strategies*; Springer International Publishing: Cham, Switzerland, 2020; pp 431–456. DOI: 10.1007/978-3-030-34475-7_19.
- (30) Chen, C.; Xie, Z.; Zhang, P.; Liu, Y.; Wang, X. Cooperative enhancement of fungal repelling performance by surface photografting of stereochemical bi-molecules. *Colloid Interface Sci. Commun.* **2021**, *40*, 100336.